Hydrological Processes

WILEY

RESEARCH ARTICLE OPEN ACCESS

Distributed Sediment Delivery at Masse Experimental Basin (Central Italy)

Vincenzo Palmeri[1,2] | Vincenzo Pampalone[1] | Francesca Todisco[3] | Lorenzo Vergni[3] | Lorenzo Verzieri[3] | Alessio Massimi Alunno[3] | Vito Ferro[1,2]

[1]Department of Agricultural, Food and Forest Sciences, University of Palermo, Palermo, Italy | [2]NBFC, National Biodiversity Future Center, Palermo, Italy | [3]Department of Agricultural, Food and Environmental Science, University of Perugia, Perugia, Italy

Correspondence: Vincenzo Pampalone (vincenzo.pampalone@unipa.it)

Received: 8 January 2026 | **Revised:** 24 February 2026 | **Accepted:** 26 February 2026

Keywords: basin management | SEDD model | sediment transport | soil conservation | soil erosion processes

ABSTRACT

The use of appropriate models for environmental decision-making is crucial for supporting soil conservation strategies, particularly in erosion-prone systems such as Mediterranean basins. In this study, the suitability of the Sediment Delivery Distributed (SEDD) model at the event scale was evaluated in a 231 ha basin in Central Italy, where rainfall–runoff–sediment yield data from four erosive events were available. The model was applied by subdividing the basin into morphological units, defined as areas with uniform aspect, length, and slope steepness. Model parameterization involved the estimation of a single coefficient, β_e, embedded in the sediment delivery ratio of each morphological unit. The variability of β_e with rainfall–runoff event intensity was analysed. The resulting relationship reflects the physical mechanism whereby sediment transport along hillslopes becomes more efficient as event intensity increases, as represented by the runoff coefficient Q_R. Analysis of the empirical cumulative frequency distribution of the sediment delivery ratio for each morphological unit suggests that the influence of the runoff coefficient on β_e may vanish during the most erosive events. Under this hypothesis, for $Q_R > 0.15$, the variability of sediment delivery processes is governed solely by the structural component of sediment connectivity, while the functional component becomes invariant and characteristic of the investigated basin.

1 | Introduction

The European Union (EU) Thematic Strategy for Soil Protection (2006) defines soil as essentially a non-renewable resource and a very dynamic system, which performs many functions and delivers services vital to human activities and ecosystem survival. This definition highlights the slow nature of soil formation, which requires hundreds to thousands of years to produce only a few centimetres of topsoil under normal agricultural conditions (Bazzoffi 2009; Di Stefano and Ferro 2016; Di Stefano et al. 2023; Carollo et al. 2023). In contrast, soil degradation due to erosion processes is rapid and often accelerated by anthropogenic activities (Lal 2014; Raclot et al. 2018).

The implementation of soil erosion control and management strategies (Cerdà et al. 2015; Mekonnen et al. 2015; Sadeghi et al. 2015) requires the optimal allocation of conservation measures within a basin and the use of models capable of estimating soil loss and sediment yield in a spatially distributed manner (Renard et al. 1994; Boardman 2006). Basin sediment yield can be estimated by coupling a gross erosion model with a mathematical operator that accounts for sediment transport efficiency along both hillslopes and the channel network (Walling 1983, 1988; Richards 1993; Atkinson 1995; Lane et al. 2000; Kothyari 2008).

The sediment delivery ratio (SDR), defined as the ratio between basin sediment yield and gross erosion, is widely used as an index of sediment transport efficiency (Walling 1983; Dickinson and Collins 1998). However, it represents a *black-box* concept and does not explicitly consider the spatial and temporal patterns of sediment transfer from source areas to the channel network (de Vente et al. 2007).

Investigating within-basin variability in sediment delivery processes requires both the subdivision of the basin into elementary spatial units (e.g., grid cells, triangular elements, or morphological units) (Di Stefano et al. 1999a, 1999b; Di Stefano, Ferro, and Porto 2000a; Di Stefano, Ferro, Porto, and Tusa 2000b; Aksoy and Kavvas 2005) and the application of a model to estimate gross erosion from each unit (Wischmeier and Smith 1978; Nearing et al. 1989; Renard et al. 1997; Morgan and Nearing 2000). Accounting for spatial variability in sediment delivery allows identification of the areas contributing most to sediment yield at the basin outlet, where conservation strategies and management interventions can be most effective.

Numerous empirical, conceptual, and physically based models are currently available for estimating soil erosion at different spatial and temporal scales (Bagarello, Ferro, and Flanagan 2018b). While process-oriented models continue to be developed (Boardman 2006; Morgan and Nearing 2000), empirical approaches such as the Universal Soil Loss Equation (USLE) and its revised version (RUSLE) remain widely used and continuously updated (Wischmeier and Smith 1978; Renard et al. 1997; Bagarello and Ferro 2004; Bagarello et al. 2011; Bagarello, Di Stefano, Ferro, and Pampalone 2018a; Bagarello, Ferro, and Flanagan 2018b; Bagarello, Ferro, Giordano, et al. 2018c; Bagarello et al. 2020; Di Stefano et al. 2017; Pampalone et al. 2023). Nearing (2013) emphasized that, for many practical applications, USLE has proven—and continues to be—a successful tool (Bagarello, Ferro, and Flanagan 2018b).

Originally designed to estimate long-term average annual soil loss due to interrill and rill erosion, USLE/RUSLE has remained popular because it combines acceptable accuracy with relative simplicity (Risse et al. 1993; Tiwari et al. 2000), requires the use of quite basic information, thus resulting attractive from a practical point of view (Morgan 2005; Bagarello et al. 2008; Gessesse et al. 2015), relies on widely available input data, and has become a standard tool in soil conservation practice (Morgan 2005).

Ferro and Minacapilli (1995) proposed coupling USLE with a spatially distributed sediment delivery ratio to estimate within-basin sediment yield (Ferro 1997; Ferro, Porto, and Tusa 1998b; Ferro and Porto 2000; Di Stefano and Ferro 2007, 2018). The resulting SEdiment Delivery Distributed (SEDD) model simulates hillslope sediment transfer from source areas to the nearest stream reach. The model's *internal functioning*, which accounts for its internal consistency, has been validated using independent techniques such as Cs^{137} (Ferro, Di Stefano, et al. 1998a; Ferro, Porto, and Tusa 1998b; Ferro et al. 2001; Di Stefano, Ferro, and Porto 2000a; Porto and Walling 2015), Be^7 tracers (Porto and Callegari 2021), and clay enrichment analysis (Di Stefano and Ferro 2002).

The SEDD model, often integrated with GIS tools (Jain and Kothyari 2000; Bhattarai and Dutta 2008), has been applied in various environmental contexts (Ali and De Boer 2010; López-Vicente et al. 2011; Taguas et al. 2011; Lee and Kang 2014; Di Stefano et al. 2016; Di Stefano and Ferro 2017a; Netti et al. 2024; Alam and Maiti 2025), both for scenario analysis (Fu et al. 2006; Batista et al. 2021) and for evaluating the effectiveness of soil conservation strategies (Fernandez et al. 2003).

In this paper, the SEDD model is first briefly presented. Subsequently, the experimental monitoring station located at the outlet of the Masse SERLAB basin near Perugia (Central Italy) is described. The station allows runoff and sediment yield to be monitored at the event scale. Finally, measurements from erosive events recorded between February 2024 and April 2025 are used to calibrate the model and analyse the dependence of the sediment delivery ratio on runoff characteristics.

In Italy, previous applicability tests of SEDD model, at event scale, were performed at Sicilian and Calabrian experimental basins (e.g., Di Stefano and Ferro 2007; Porto and Walling 2015; Porto and Callegari 2021) with a Mediterranean climate (rainfall occurring in autumn and winter). This paper focuses on SEDD applicability in Central Italy, which is characterized by a different sub-continental rainfall regime (rainfalls primarily occurring in autumn and spring).

2 | Materials and Methods

2.1 | Masse Experimental Basin

The Masse basin is located in a hilly area of the municipality of Marsciano (Perugia, Central Italy) and covers an area of 231 ha (Figure 1). The Digital Elevation Model (DEM) used in this study has a spatial resolution of 10 m, providing a suitable balance between accuracy and computational efficiency. The DEM was derived from the national raster dataset Tinitaly 1.1 (Tarquini et al. 2023).

The basin elevation ranges from 290.9 to 212.7 m a.s.l. at the outlet section, where a small reservoir is located. The average hillslope gradient is 9.5%, and the total length of the main stream is approximately 2.3 km (Figure 1).

Land use information was obtained through an integrated analysis of satellite imagery, surveys, and field investigations, supported by direct knowledge of the Masse watershed. Three main land use categories were identified: agricultural land, water bodies, and urbanised areas. Agricultural land dominates the basin and is mainly characterised by herbaceous crops following an autumn–winter cycle, such as cereals and leguminous crops, particularly fava beans. Permanent crops, including vineyards and olive groves, are also present. The

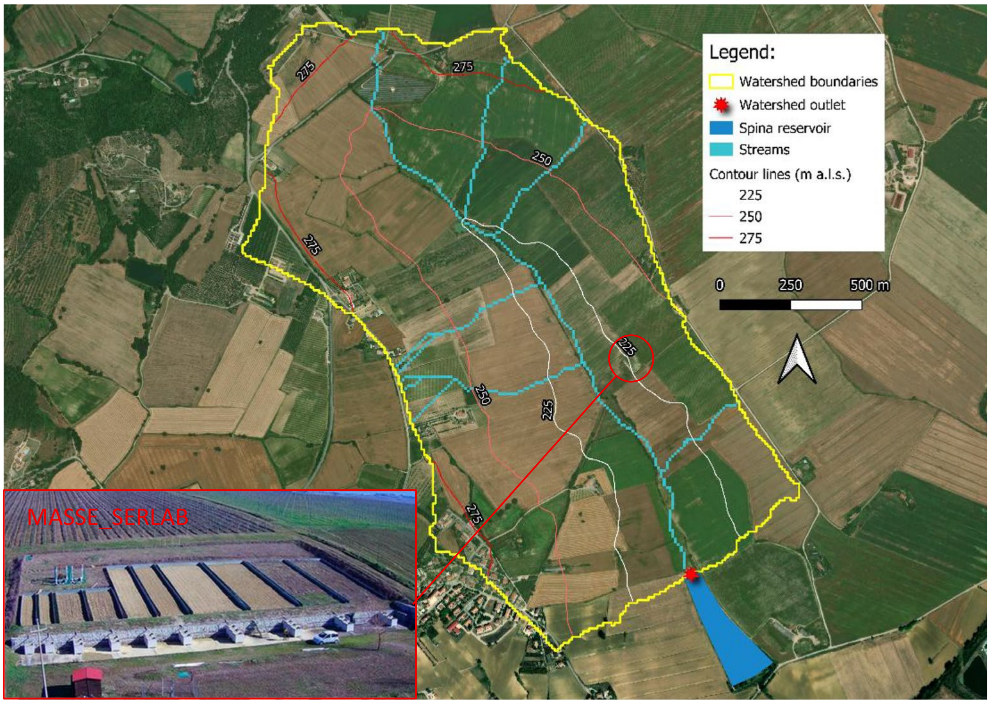

FIGURE 1 | Map of the Masse basin (PG, Italy), showing the basin boundaries, stream network, contour lines, outlet, and reservoir position. The sub-panel shows the Wischmeier-type plots of the Masse_SERLAB.

predominance of seasonal crops results in extended periods during which the soil remains bare, thereby increasing its susceptibility to erosion. Tillage operations are generally carried out along the direction of maximum slope, and no soil conservation practices are implemented. Urbanised areas occupy only a small fraction of the basin.

At the basin outlet, a diversion channel branches from the main stream and conveys a portion of the runoff towards a sedimentation basin located upstream of a small reservoir. The sedimentation basin functions as a physical filter by promoting the settling of suspended sediments, thereby reducing the sedimentation rate within the reservoir. Despite this mitigation effect, the reservoir has progressively experienced siltation, resulting in a significant reduction of its effective storage capacity. A bathymetric survey conducted in May 2024 indicated that the maximum depth near the dam, which has a height of 5 m, has decreased to approximately 1.3 m. The reservoir depth decreases almost linearly upstream, reaching about 0.8 m in the uppermost area, where riparian wood vegetation is present.

To model the spatial variability of sediment delivery processes, the basin was subdivided into morphological units (Ferro and Minacapilli 1995). These units are defined as areas with uniform slope and aspect, known hillslope length, land use, and soil type, and are bound downslope either by a change in slope or by an element intercepting surface runoff (Figure 2).

A systematic soil sampling campaign was conducted within each morphological unit (Figure 2) to determine particle size distribution and total organic carbon content. For units larger than 5 ha, two samples were collected to capture internal variability, whereas one sample per unit was collected for smaller units to ensure adequate spatial representation.

2.2 | Sediment Yield Monitoring at the Masse Station

The Masse basin hosts the Masse SERLAB monitoring station (Figure 1), dedicated to the study of soil erosion processes in hilly environments. The station has been operational since 2008 (Todisco et al. 2012) and includes Wischmeier-type erosion plots and a fully equipped weather station. Recorded meteorological variables include precipitation, air temperature, global solar radiation, wind speed, and relative humidity. Rainfall data are available at a 5-min temporal resolution.

Since September 2023, flow discharge and sediment concentration have been monitored at the basin outlet (Figure 3), located immediately upstream of the diversion channel leading to the sedimentation basin. The monitoring cross-section has a trapezoidal shape, with a bottom width of 0.85 m and a depth of 1.05 m. The side banks form angles of 39° and 41° with the vertical, resulting in a top width of 2.60 m. Routine maintenance is performed every 2–3 years to reshape the cross-section, control morphological evolution, and ensure stable hydraulic conditions. The channel bed consists mainly of silty and clayey materials. During autumn and winter, when vegetation is absent, the hydraulic behavior of the banks resembles that of bare or sparsely vegetated soils.

Mean flow velocity and water depth are measured using a SonTek FlowTracker2 Handheld ADV, allowing the development of the stage–discharge relationship. Under uniform flow conditions, application of Chezy's equation yielded a Manning roughness coefficient of 0.107.

Flow depth is also continuously monitored using a relative pressure probe (DS(T) 22, SEBA Hydrometrie GmbH & Co. KG) installed in the measurement channel. To optimise data acquisition, the sensor operates with an event-based sampling frequency: one measurement per hour for water levels below 0.15 m and one measurement every 10 min for levels exceeding this threshold. During the recession limb of a flood event, a hysteresis value of 0.05 m is applied, maintaining the 10-min sampling interval until the water level drops below 0.10 m. All measurements represent instantaneous values at the time of acquisition.

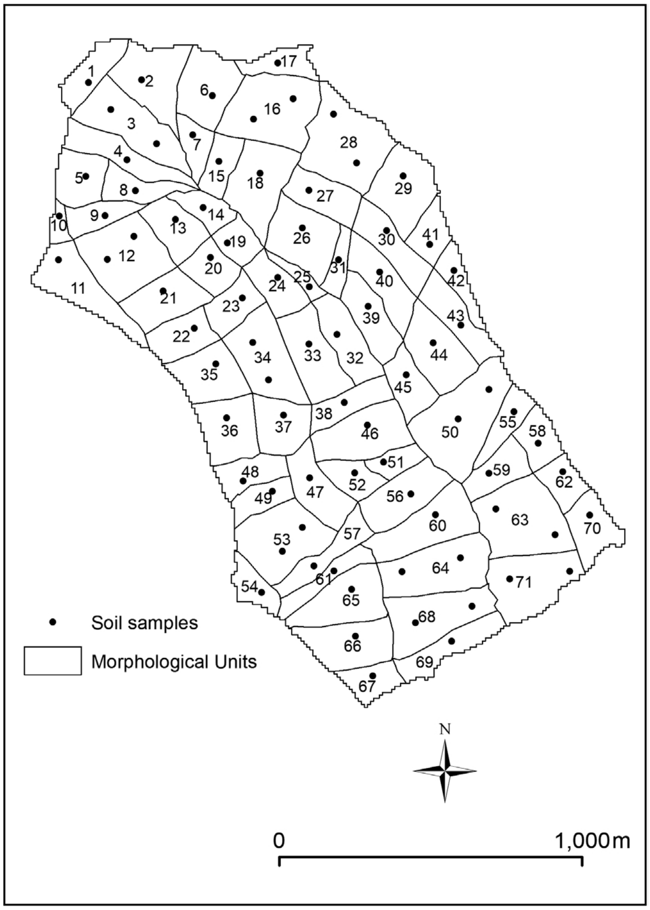

FIGURE 2 | Discretization of the Masse basin into morphological units and locations of the 82 collected soil samples.

Sediment concentration is determined through the analysis of water samples collected using a Teledyne ISCO 3700 portable sampler installed at the outlet section (Figure 3). The sampler can collect up to 24 discrete samples and is fully programmable for both sequential and composite sampling. An actuator automatically triggers sampling when the flow depth reaches the probe. The system was installed in September 2023 and programmed to initiate sampling when the flow depth exceeds 0.20 m above the channel bed. Five subsamples are collected per bottle, each with a constant volume of 150 mL and a sampling interval of 4 min. Consequently, each bottle contains 750 mL and represents runoff collected over a 20-min interval. Sediment concentration is therefore measured at a frequency of three samples per hour during flood events only. This temporal resolution is adequate for capturing the dynamics of rapid flood events typical of the Masse basin, which has a concentration time of approximately 1 h. Sampling continues for up to 8 h, corresponding to the sampler's maximum capacity.

To determine sediment concentration, each sample is weighed and oven-dried at 105°C for 48 h until a constant mass is reached. The water volume is obtained by subtracting the dry sediment mass from the total sample weight, assuming a water density of 1000 $\mathrm{kg\,m^{-3}}$ at 20°C. The suspended sediment concentration (SSC, $\mathrm{g\,L^{-1}}$) is calculated as the ratio between dry sediment mass and water volume. Each SSC value represents the average concentration over the 20-min sampling interval. The product of SSC and flow discharge Q yields the sediment discharge Q_s, enabling a detailed reconstruction of the temporal evolution of suspended sediment yield during storm events.

Flow discharge and SSC data were resampled to a 1-min temporal resolution and merged into a single dataset. Data gaps were filled as follows: (i) prior to flood onset, discharge values recorded at hourly intervals were assumed constant between consecutive measurements; during flood events, discharge values recorded every 10 min were averaged between consecutive observations and assigned to the first minute of the interval, remaining constant for the subsequent 9 min; (ii) sediment concentration was assumed constant over the 20 min preceding each sampling time.

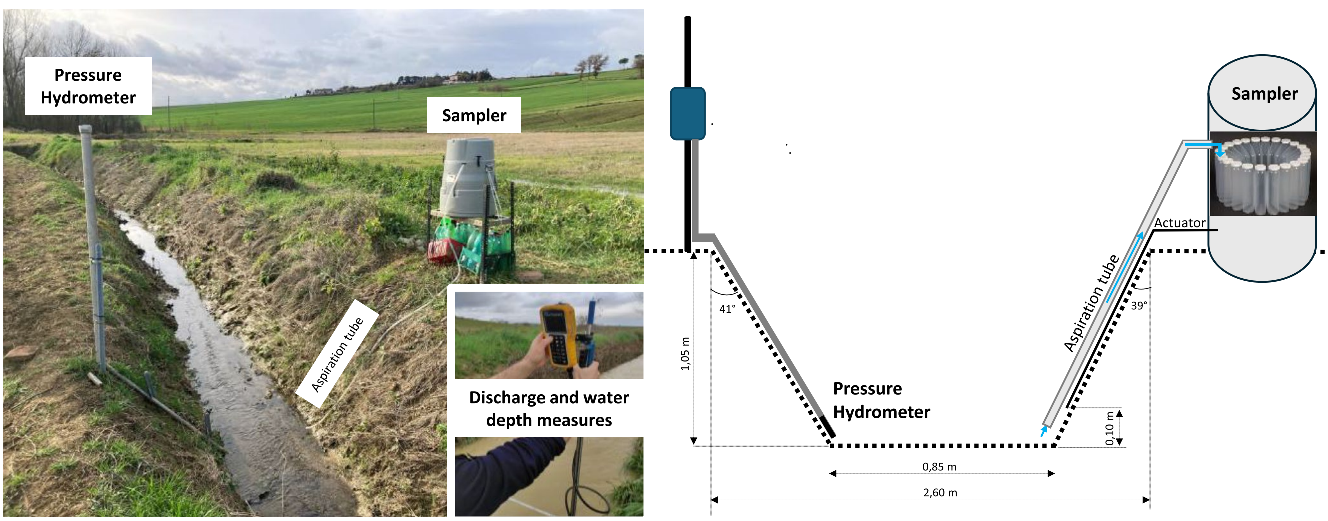

FIGURE 3 | View and scheme of the sediment yield and flow discharge monitoring station.

2.3 | Estimate of Gross Erosion

At the event scale, soil loss was estimated using the USLE/RUSLE formulation (Wischmeier and Smith 1978):

$$A_e = EI_{30} K L S C P \tag{1}$$

where A_e (Mg ha^{-1}) is the event soil loss; EI_{30} (MJ mm ha^{-1} h^{-1}) is the rainfall erosivity factor, defined as the product of rainfall kinetic energy E (MJ ha^{-1}) and the maximum 30-min rainfall intensity I_{30} (mm h^{-1}); K (Mg ha^{-1} per unit of EI_{30}) is the soil erodibility factor; L and S are the slope length and slope steepness factors, respectively; C is the cover-management factor; and P is the support practice factor.

Currently, the USLE is widely applied in Europe and in many other Mediterranean countries for practical purposes (Bagarello and Ferro 2004; Morgan 2005; Bagarello et al. 2008, 2010). Previous studies verified the applicability of USLE-type models and established their performance (Todisco et al. 2015; Bagarello, Ferro, Giordano, et al. 2018c; Bagarello, Ferro, Pampalone, et al. 2018d) at Masse SERLAB monitoring station (Figure 1). A lack of ability of the USLE to predict event soil loss can be expected given that the rainfall erosivity factor EI_{30} does not consider runoff explicitly, and specific investigations (Todisco et al. 2015, 2022; Bagarello et al. 2018c, 2018d) pointed out that using a rainfall–runoff erosivity factor (e.g., correcting EI_{30} by runoff coefficient or soil moisture) enhances the USLE capability to account for variations in event soil losses. A rainfall-runoff erosivity factor is also able to take into account transport and deposition of soil particles that in the SEDD model are considered by the sediment delivery ratio of each morphological unit. In other words, combining USLE and sediment delivery ratio is expected to consider both transport and deposition phenomena.

The slope length factor L was calculated as (Moore and Burch 1986; Moore and Wilson 1992; Di Stefano, Ferro, and Porto 2000a):

$$L = \left(\frac{\lambda}{22.1}\right)^m \tag{2}$$

where λ is the slope length and m is an exponent related to the ratio F between rill and interrill erosion:

$$m = \frac{F}{1+F} \tag{3}$$

$$F = \frac{\frac{\sin\theta}{0.0896}}{3(\sin\theta)^{0.8} + 0.56} \tag{4}$$

where θ is the slope angle.

The slope steepness factor S was computed using the Nearing (1997) equation:

$$S = -1.5 + \frac{17}{1 + \exp\left(2.3 - 6.1 \sin\theta\right)} \tag{5}$$

The soil erodibility factor K was estimated using the Wischmeier–Johnson–Cross method (Wischmeier et al. 1971; Bagarello and Ferro 2006) based on 82 soil samples distributed across the basin (Figure 2).

The cover-management factor C was assigned according to land use (Bagarello and Ferro 2006): 0.23 for autumn–winter herbaceous crops (cereals and legumes), 0.04 for olive groves with herbaceous cover, 0.02 for vineyards, and 0.007 for forested areas. The difficulties in explaining the temporal variability of the crop factor for olive, vineyard and forested areas (Cinnirella et al. 1998) can be justified taking into account that the overall erosion-reducing effectiveness of these crops not only depends on the type of vegetation and its growth but also on how much of the erosive rain occurs during the least crop protection. The interrelation between crop effectiveness and climate was neglected and a constant value of C was assumed to avoid the introduction of uncertainties related to a more detailed estimate procedure. In the future, when more erosive events will be available, the C factor estimate could be improved using some erosive events for calibration. Detailed information on the surface coverage variability and the corresponding soil loss ratio should be strictly required to estimate the C factor at event scale for herbaceous crops. At present, seasonal variations in herbaceous crops were neglected, as they are minimal during the October–February period, when most events occurred, and to avoid introducing additional uncertainty (Bagarello and Ferro 2006). Since no soil conservation practices are implemented in the basin, the support practice factor P was set equal to 1.

2.4 | Estimate of Distributed Sediment Delivery Processes

At the hillslope scale, within-basin sediment yield variability was modelled following the sequential Lagrangian approach proposed by Ferro and Minacapilli (1995), which tracks sediment transport from each morphological unit to the nearest stream reach using a unit-specific sediment delivery coefficient (Novotny and Chesters 1989).

In small basins lacking well-developed floodplains (Walling et al. 1986) and with ephemeral channels, sediment deposition within the channel network (the "channel component") can be neglected (Walling 1983, 1988; Richards 1993; Atkinson 1995). Under this assumption, the sediment delivery ratio SDR_i of each morphological unit i depends on the travel time $t_{p,i}$ of sediment particles along the hydraulic pathway from the source area to the nearest stream reach (Ferro and Minacapilli 1995).

The travel time $t_{p,i}$ is computed as the sum of travel times across all morphological units located along the hydraulic path:

$$t_{p,i} = \sum_{j=1}^{N_p} \frac{\lambda_{i,j}}{\sqrt{s_{i,j}}} \tag{6}$$

where N_p is the number of morphological units along the path, and $\lambda_{i,j}$ and $s_{i,j}$ are the length and slope of the jth unit. Ferro (1997) and Ferro and Minacapilli (1995) showed that the sediment delivery ratio can be expressed as:

$$SDR_i = \exp\left(-\beta\, t_{p,i}\right) = \exp\left[-\beta \sum_{j=1}^{N_p} \frac{\lambda_{i,j}}{\sqrt{s_{i,j}}}\right] \tag{7}$$

TABLE 1 | Characteristic data of the monitored rainfall–runoff events.

Event	EI_{30} (MJ mm ha^{-1} h^{-1})	P_e (mm)	Q_R (–)	$Y_{m,e}$ (Mg)	β_e (m^{-1})	μ (SDR_i)	σ (SDR_i)	$SDR_{b,e}$ (–)
2024/02/13–25	115.0	36.8	0.155	42.9	0.00264	0.0847	0.1250	0.060
2024/10/03	150.3	59.6	0.021	6.27	0.00598	0.0175	0.0593	0.0067
2024/12/20	94.1	28.8	0.285	37.4	0.00256	0.0891	0.1276	0.064
2025/04/23	35.4	18.2	0.071	5.79	0.00372	0.0456	0.09526	0.026

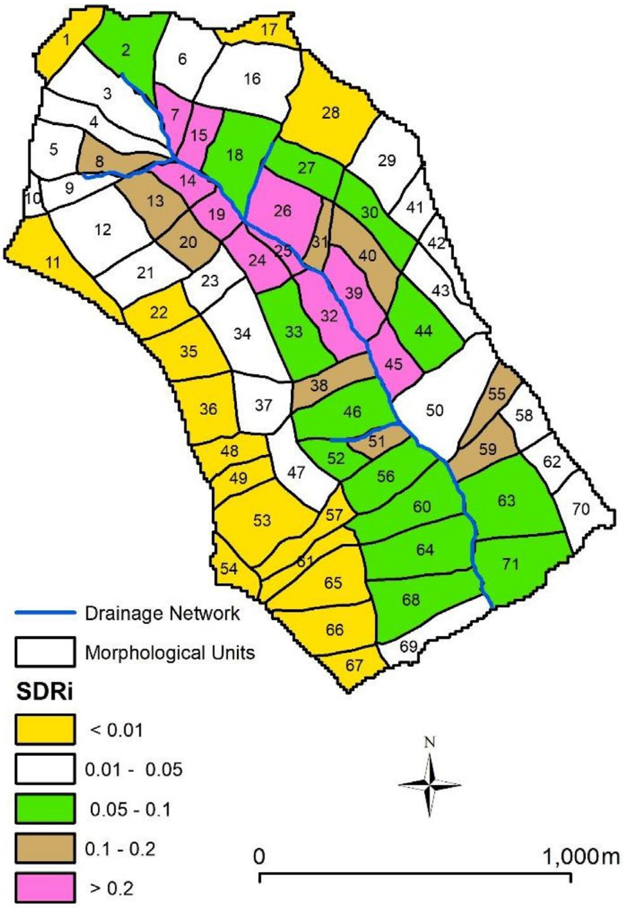

FIGURE 4 | Spatial distribution of SDR_i for the rainfall event 2024/12/20.

where β is a coefficient characteristic of the basin and the temporal scale considered (annual or event). Therefore, SDR_i is composed by two terms: the travel time, which is a time invariant morphological variable (Equation 6), and the coefficient β that is time dependent (i.e., it varies annually or with the considered rainfall event).

For a basin discretized into N_u morphological units, the event-scale sediment yield at the basin outlet $Y_{s,e}$ (Mg) is obtained from the sediment balance equation:

$$Y_{s,e} = \sum_{i=1}^{N_u} A_i \, SDR_i \, S_{u,i} = EI_{30} \sum_{i=1}^{N_u} K_i L_i S_i C_i P_i \exp\left(-\beta_e t_{p,i}\right) S_{u,i} \tag{8}$$

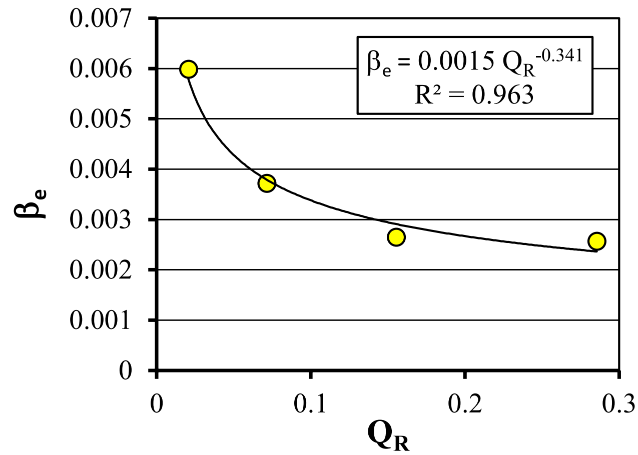

FIGURE 5 | Relationship between the coefficient β_e and the runoff coefficient Q_R for the investigated Masse basin.

where A_i (Mg ha^{-1}) is the soil loss from the ith morphological unit estimated by USLE/RUSLE; K_i, L_i, S_i, C_i, and P_i are the corresponding USLE/RUSLE factors; $S_{u,i}$ (ha) is the unit area; and $\beta = \beta_e$ is the single event-scale parameter of the SEDD model.

Four event-scale sediment yields ($Y_{m,e}$) measured at the outlet of the experimental basin were available for calibrating the SEDD model. The event-scale parameter β_e was estimated using Equation (8), adopting the measured EI_{30} values and imposing $Y_{s,e} = Y_{m,e}$.

3 | Results

For each event, Table 1 reports the values of EI_{30}, rainfall amount P_e, runoff coefficient Q_R, measured sediment yield $Y_{m,e}$ and the corresponding β_e, the mean $\mu(SDR_i)$ and standard deviation $\sigma(SDR_i)$ of SDR_i, and the basin-scale sediment delivery ratio $SDR_{b,e}$. The latter was computed for each event as the ratio between the measured sediment yield and the gross erosion estimated by the USLE.

The spatial distribution of SDR_i is plotted, as an example, in Figure 4 for the rainfall event 2024/12/20, which is characterised by the highest $SDR_{b,e}$.

In agreement with previous studies (Di Stefano et al. 2019; Bagarello et al. 2020; Pampalone et al. 2023), the relationship between β_e and Q_R was investigated. Figure 5 shows that β_e never approaches zero, clearly indicating that sediment delivery processes must be accounted for when estimating basin sediment yield. In other words, when gross erosion is estimated using the event rainfall erosivity factor EI_{30}, a correction is required to account for sediment transport and deposition processes along hillslopes.

The variability of β_e can be explained by the basin runoff coefficient Q_R according to the following relationship (Figure 5):

$$\beta_e = 0.0015\, Q_R^{-0.341} \tag{9}$$

Consistent with previous findings (Di Stefano and Ferro 2017b), Equation (9) reflects the physical mechanism whereby sediment transport along hillslopes becomes increasingly efficient as event intensity, represented by the runoff coefficient, increases.

For the four analysed events, Figure 6 presents the cumulative empirical frequency distributions of the sediment delivery ratio SDR_i. The results confirm that the highest SDR_i values correspond to the event of 20 December 2024, which is characterised by the highest measured runoff coefficient ($Q_R = 0.285$; Table 1). Conversely, the lowest SDR_i values are associated with the 3 October 2024 event, which exhibited the minimum runoff coefficient ($Q_R = 0.021$; Table 1).

The statistical descriptors of the SDR_i distributions, namely the mean $\mu(SDR_i)$ and the standard deviation $\sigma(SDR_i)$, reported in Table 1, are plotted as a function of Q_R in Figure 7. Both parameters tend to become nearly constant for $Q_R > 0.155$, as a result of the substantial overlap between the distributions corresponding to the 13–25 February 2024 and 20 December 2024 events.

Finally, as shown in Figure 8, $SDR_{b,e}$ increases with increasing rainfall–runoff event intensity, confirming the nearly invariance of sediment delivery processes ($SDR_{b,e}$ = constant) under more intense hydrological conditions.

4 | Discussion

The decreasing β_e–Q_R relationship indicates that event-scale sediment delivery processes become less limiting as hillslope flow discharge increases, leading to higher SDR_i values for increasing runoff coefficients. Within the SEDD framework, gross erosion for each morphological unit is estimated using the USLE, which

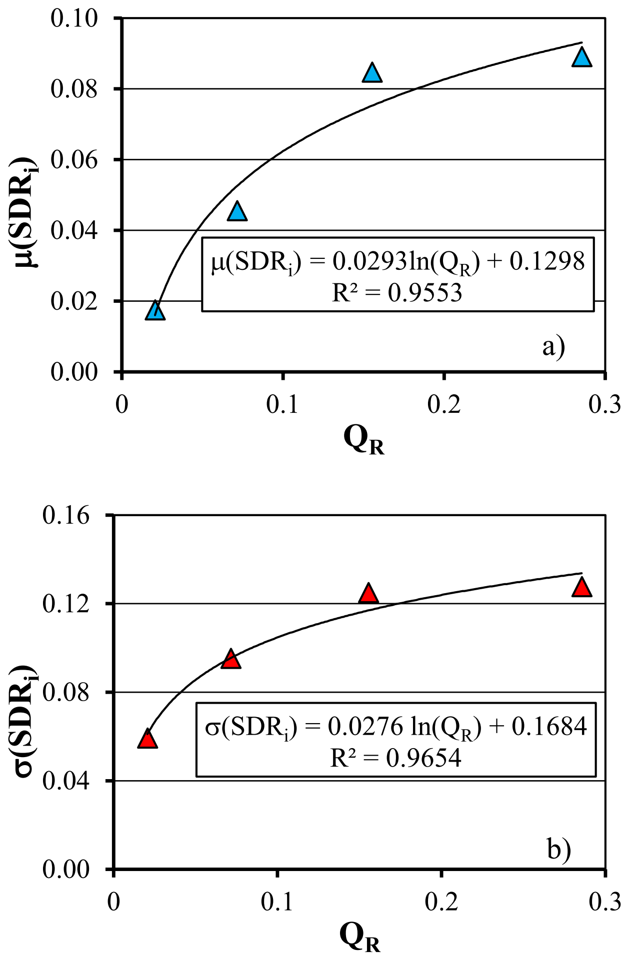

FIGURE 7 | Relationship between the statistical parameters (mean $\mu(SDR_i)$ (a) and standard deviation $\sigma(SDR_i)$ (b)) and the event runoff coefficient Q_R.

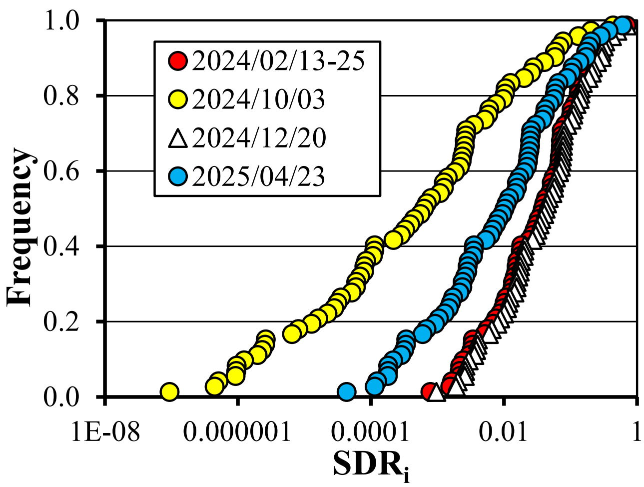

FIGURE 6 | Empirical cumulative frequency distributions of SDR_i for the investigated events.

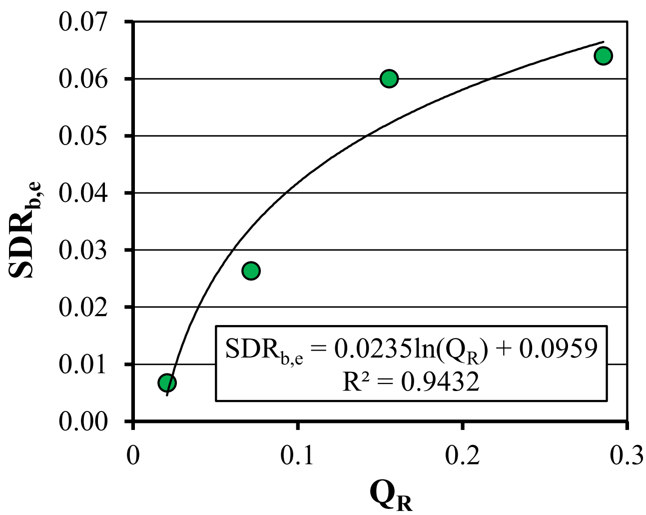

FIGURE 8 | Relationship between the basin sediment delivery ratio $SDR_{b,e}$ and the runoff coefficient Q_R.

assumes that soil loss is not constrained by the runoff capacity to transport detached particles, that is, a transport-unlimited condition (Bagarello, Di Stefano, Ferro, and Pampalone 2018a). In contrast, sediment yield is controlled by the transport capacity T_c of surface runoff.

The soil loss estimated by the USLE can therefore be attenuated through the sediment delivery ratio SDR_i, which is linked to T_c and allows deposition processes to be accounted for when the sediment load exceeds T_c. Since transport capacity increases with flow discharge (Ferro 1998), SDR_i is directly related to hillslope runoff and, consequently, to the runoff coefficient Q_R, as confirmed by the results shown in Figure 5.

These findings can also be interpreted through the concept of sediment connectivity, which distinguishes between structural and functional components (Di Stefano and Ferro 2017b; Najafi et al. 2021; Shi et al. 2025). Sediment connectivity describes "the pathways, processes and probability of sediment transfer from sources to potential sinks within a given watershed" (Shi et al. 2025) and represents an effective metric for assessing soil erosion and sediment yield processes at the basin scale (Bracken et al. 2015). Within the SEDD framework, the sediment delivery ratio SDR_i can be regarded as a measure of overall sediment connectivity.

The structural component of connectivity is independent of the temporal scale and depends on the subdivision of the basin into morphological units and on their geometric characteristics, such as slope length, steepness, and travel time. Conversely, the functional component is event-dependent and is represented by the coefficient β_e. The present analysis, particularly the relationship expressed by Equation (9), demonstrates that sediment delivery ratios increase, sediment transport efficiency along hillslopes increases, and overall sediment connectivity becomes stronger as event intensity—represented by Q_R—increases.

Figure 5 further indicates that the two most erosive events (13–25 February 2024 and 20 December 2024), characterised by the highest runoff coefficients, exhibit similar β_e values. This suggests the existence of a threshold runoff coefficient, estimated for the Masse basin to be approximately $Q_R = 0.15$, above which β_e becomes effectively constant. This hypothesis will require verification through the observation of additional events with $Q_R > 0.15$.

As a consequence of an invariant β_e, the cumulative frequency distributions corresponding to the highest SDR_i values (Figure 6) for the 13–25 February 2024 and 20 December 2024 events, characterised by Q_R values of 0.155 and 0.285, respectively, nearly overlap. If confirmed by further measurements, this behaviour would imply that, for events with $Q_R > 0.15$, the functional component of sediment connectivity becomes invariant, and the variability of SDR_i is governed solely by the structural component of the basin. In this case, the functional connectivity would represent an intrinsic characteristic of the investigated basin.

Independent evidence supporting this hypothesis is provided by plot-scale measurements at Masse SERLAB (Figure 1), where Todisco et al. (2022) identified thresholds of rainfall depth and antecedent soil moisture content, derived from satellite data, associated with runoff rates. All runoff coefficients exceeding these thresholds were greater than 0.1, with most values exceeding 0.15. If these findings are confirmed at the basin scale, rainfall depth and antecedent soil moisture thresholds could be used to identify events for which the functional connectivity component is invariant (β_e = constant) in the Masse basin.

Finally, when sediment delivery processes are represented by a lumped index such as the basin-scale sediment delivery ratio $SDR_{b,e}$, the results shown in Figure 8 suggest that this index may also be considered invariant for events with $Q_R > 0.15$. Under these conditions, the basin response in terms of sediment delivery would be governed primarily by morphological controls and would be directly related to the distribution of slope length and steepness of the morphological units into which the basin is subdivided.

5 | Conclusions

The optimal allocation of soil conservation strategies within a basin requires an accurate assessment of the spatial variability of sediment delivery processes through distributed modelling approaches. In this study, the SEdiment Delivery Distributed (SEDD) model, which explicitly accounts for sediment deposition along hydraulic pathways, was applied at the event scale to the Masse experimental basin. Application of the SEDD model requires the estimation of a single parameter, β_e, which governs the sediment delivery ratio of each morphological unit.

Model calibration based on four rainfall–runoff events monitored at the basin outlet allowed the relationship between β_e and the runoff coefficient to be quantified. This relationship reflects the physical mechanism whereby sediment transport along hillslopes becomes increasingly efficient as event intensity, represented by the runoff coefficient, increases.

Analysis of the empirical cumulative frequency distributions of the sediment delivery ratio for individual morphological units indicates that the influence of the runoff coefficient on β_e becomes negligible for the most erosive events. Under this hypothesis, for events characterised by $Q_R > 0.15$, variability in sediment connectivity is controlled exclusively by the structural component, while the functional component becomes invariant and representative of the basin. Consequently, for high-intensity rainfall–runoff events ($Q_R > 0.15$), sediment delivery processes appear to be governed primarily by morphological attributes such as slope length and steepness, as β_e assumes a constant value.

Given the limited number of available sediment yield measurements, additional rainfall–runoff events should be monitored to further test and strengthen these conclusions and to confirm the existence and robustness of the identified runoff coefficient threshold.

Acknowledgments

Open access publishing facilitated by Universita degli Studi di Palermo, as part of the Wiley - CRUI-CARE agreement.

Funding

This study was carried out within the PRIN 2022 "Soil Conservation for sustainable AgricuLture in the framework of the European green deal" (SCALE), Project code 2022PB2NSP, CUP B53D23017980006 and received funding from the European Union Next-GenerationEU (National Recovery and Resilience Plan-NRRP, Mission 4, Component 2, Investment 1.1) and within the European Union-Next-GenerationEU-National Recovery and Resilience Plan (NRRP)–MISSION 4 COMPONENT 2, INVESTIMENT N. 1.1, CALL PRIN 2022 D.D. 104 02-02-2022–(Small reservoIrs restoration: Green blu-infrastructures to enHance rural area resilience To clImate chaNGe—SIGHTING) CUP N. J53D23002910006.

Data Availability Statement

The data that support the findings of this study are available from the corresponding author upon reasonable request.

References

Aksoy, H., and M. L. Kavvas. 2005. "A Review of Hillslope and Watershed Scale Erosion and Sediment Transport Models." *Catena* 64: 247–271.

Alam, S. K., and R. Maiti. 2025. "Identifying Soil Erosion Hotspot: Sediment Delivery Ratio Modelling." In *Sediment Source to Sink: Deciphering Sediment Connectivity to Large Dams in Damodar River Basin*, 59–86. Springer.

Ali, K. F., and D. H. De Boer. 2010. "Spatially Distributed Erosion and Sediment Yield Modeling in the Upper Indus River Basin." *Water Resources Research* 46, no. 8: W08504.

Atkinson, E. 1995. "Methods for Assessing Sediment Delivery in River Systems." *Journal of Hydrological Sciences* 40, no. 2: 273–280.

Bagarello, V., G. V. Di Piazza, V. Ferro, and G. Giordano. 2008. "Predicting Unit Plot Soil Loss in Sicily, South Italy." *Hydrological Processes* 22: 586–595.

Bagarello, V., C. Di Stefano, V. Ferro, et al. 2011. "Predicting Soil Loss on Moderate Slopes Using an Empirical Model for Sediment Concentration." *Journal of Hydrology* 400: 267–273.

Bagarello, V., C. Di Stefano, V. Ferro, and V. Pampalone. 2018a. "Comparing Theoretically Supported Rainfall-Runoff Erosivity Factors at the Sparacia (South Italy) Experimental Site." *Hydrological Processes* 32: 507–515.

Bagarello, V., and V. Ferro. 2004. "Plot-Scale Measurement of Soil Erosion at the Experimental Area of Sparacia (Southern Italy)." *Hydrological Processes* 18: 141–157.

Bagarello, V., and V. Ferro. 2006. *Soil Erosion and Conservation*, 540. McGraw-Hill (In Italian).

Bagarello, V., V. Ferro, and D. Flanagan. 2018b. "Predicting Plot Soil Loss by Empirical and Process-Oriented Approaches. A Review." *Journal of Agricultural Engineering* 49: 1–18.

Bagarello, V., V. Ferro, and G. Giordano. 2010. "Testing Alternative Erosivity Indices to Predict Event Soil Loss From Bare Plots in Southern Italy." *Hydrological Processes* 24: 789–797.

Bagarello, V., V. Ferro, G. Giordano, F. Mannocchi, F. Todisco, and L. Vergni. 2018c. "Statistical Check of USLE-M and USLE-MM to Predict Bare Plot Soil Loss in Two Italian Environments." *Land Degradation and Development* 29, no. 8: 2614–2628.

Bagarello, V., V. Ferro, V. Pampalone, P. Porto, F. Todisco, and L. Vergni. 2018d. "Predicting Soil Loss in Central and South Italy With a Single USLE-MM Model." *Journal of Soils and Sediments* 18, no. 12: 3365–3377.

Bagarello, V., V. Ferro, and V. Pampalone. 2020. "A Comprehensive Analysis of Universal Soil Loss Equation Based Models at the Sparacia Experimental Area." *Hydrological Processes* 34: 1545–1557.

Batista, P. V., J. P. Laceby, J. Davies, et al. 2021. "A Framework for Testing Large-Scale Distributed Soil Erosion and Sediment Delivery Models: Dealing With Uncertainty in Models and the Observational Data." *Environmental Modelling & Software* 137: 104961.

Bazzoffi, P. 2009. "Soil Erosion Tolerance and Water Runoff Control: Minimum Environmental Standards." *Regional Environmental Change* 9: 169–179.

Bhattarai, R., and D. Dutta. 2008. "A Comparative Analysis of Sediment Yield Simulation by Empirical and Process-Oriented Models in Thailand." *Hydrological Sciences Journal* 53, no. 6: 1253–1269.

Boardman, J. 2006. "Soil Erosion Science: Reflections on the Limitations of Current Approaches." *Catena* 68, no. 2–3: 73–86.

Bracken, L. J., L. Turnbull, J. Wainwright, and P. Bogaart. 2015. "Sediment Connectivity: A Framework for Understanding Sediment Transfer at Multiple Scales." *Earth Surface Processes and Landforms* 40, no. 2: 177–188.

Carollo, F. G., C. Di Stefano, A. Nicosia, V. Palmeri, V. Pampalone, and V. Ferro. 2023. "A New Strategy to Assure Compliance With Soil Loss Tolerance at a Regional Scale." *Catena* 223: 106945.

Cerdà, A., O. González-Pelayo, A. Giménez-Morera, et al. 2015. "The Use of Barley Straw Residues to Avoid High Erosion and Runoff Rates on Persimmon Plantations in Eastern Spain Under Low Frequency—High Magnitude Simulated Rainfall Events." *Soil Research* 54: 154–165.

Cinnirella, S., F. Iovino, P. Porto, and V. Ferro. 1998. "Anti-Erosive Effectiveness of Eucalyptus Coppices Through the Cover Management Factor Estimate." *Hydrological Processes* 12, no. 4: 635–649.

Communication from the Commission to the Council, the European Parliament, the European Economic and Social Committee and the Committee of the Regions. 2006. *Thematic Strategy for Soil Protection*. https://eur-lex.europa.eu/legal-content/EN/TXT/?uri=celex:52006DC0231.

de Vente, J., J. Poesen, M. Arabkhedri, and G. Verstraeten. 2007. "The Sediment Delivery Problem Revisited." *Progress in Physical Geography* 31: 155–178.

Di Stefano, C., and V. Ferro. 2002. "Linking Clay Enrichment and Sediment Delivery Processes." *Biosystems Engineering* 81, no. 4: 465–479.

Di Stefano, C., and V. Ferro. 2007. "Evaluation of the SEDD Model for Predicting Sediment Yield at the Sicilian Experimental SPA2 Basin." *Earth Surface Processes and Landforms* 32: 1094–1109.

Di Stefano, C., and V. Ferro. 2016. "Establishing Soil Loss Tolerance: An Overview." *Journal of Agricultural Engineering* XLVII: 127–133.

Di Stefano, C., and V. Ferro. 2017a. "Testing Sediment Connectivity at the Experimental SPA2 Basin, Sicily (Italy)." *Land Degradation & Development* 28, no. 7: 1992–2000.

Di Stefano, C., and V. Ferro. 2017b. "Testing the Modified Sediment Delivery Model (MOSEDD) at SPA2 Experimental Basin, Sicily (Italy)." *Land Degradation & Development* 28, no. 5: 1557–1567.

Di Stefano, C., and V. Ferro. 2018. "Modelling Sediment Delivery Using Connectivity Components at the Experimental SPA2 Basin, Sicily (Italy)." *Journal of Mountain Science* 15, no. 9: 1868–1880.

Di Stefano, C., V. Ferro, M. Burguet, and E. V. Taguas. 2016. "Testing the Long Term Applicability of USLE-M Equation at a Olive Orchard Micro Catchment in Spain." *Catena* 147: 71–79.

Di Stefano, C., V. Ferro, and V. Pampalone. 2017. "Applying the USLE Family of Models at the Sparacia (South Italy) Experimental Site." *Land Degradation and Development* 28: 994–1004.

Di Stefano, C., V. Ferro, and P. Porto. 1999a. "Modelling Sediment Delivery Processes by a Stream Tube Approach." *Hydrological Sciences Journal* 44, no. 5: 725–742.

Di Stefano, C., V. Ferro, and P. Porto. 1999b. "Linking Sediment Yield and Caesium-137 Spatial Distribution at Basin Scale." *Journal of Agricultural Engineering Research* 74: 41–62.

Di Stefano, C., V. Ferro, and P. Porto. 2000a. "Length Slope Factors for Applying the Revised Universal Soil Loss Equation at Basin Scale in Southern Italy." *Journal of Agricultural Engineering Research* 75: 349–364.

Di Stefano, C., V. Ferro, P. Porto, and G. Tusa. 2000b. "Slope Curvature Influence on Soil Erosion and Deposition Processes." *Water Resources Research* 36: 607–617.

Di Stefano, C., A. Nicosia, V. Pampalone, and V. Ferro. 2023. "Soil Loss Tolerance in the Context of the European Green Deal." *Heliyon* 9, no. 1: e12869.

Di Stefano, C., V. Pampalone, F. Todisco, L. Vergni, and V. Ferro. 2019. "Testing the Universal Soil Loss Equation-MB Equation in Plots in Central and South Italy." *Hydrological Processes* 33, no. 18: 2422–2433.

Dickinson, A., and R. Collins. 1998. "Predicting Erosion and Sediment Yield at the Catchment Scale." In *Soil Erosion at Multiple Scales, Principles and Methods for Assessing Causes and Impacts*, edited by F. W. T. Penning de Vries, F. Agus, and J. Kerr, 317–342. Cab International.

Fernandez, C., J. Q. Wu, D. K. McCool, and C. O. Stöckle. 2003. "Estimating Water Erosion and Sediment Yield With GIS, RUSLE, and SEDD." *Journal of Soil and Water Conservation* 58, no. 3: 128–136.

Ferro, V. 1997. "Further Remarks on a Distributed Approach to Sediment Delivery." *Journal of Hydrological Sciences* 42, no. 5: 633–648.

Ferro, V. 1998. "Evaluating Overland Flow Sediment Transport Capacity." *Hydrological Processes* 12, no. 12: 1895–1910.

Ferro, V., V. Bagarello, C. Di Stefano, G. Giordano, and P. Porto. 2001. "Monitoring and Predicting Sediment Yield in a Small Sicilian Basin." *Transactions of the American Society of Agricultural Engineers* 44, no. 3: 585–595.

Ferro, V., C. Di Stefano, G. Giordano, and S. Rizzo. 1998a. "Sediment Delivery Processes and the Spatial Distribution of Caesium-137 in a Small Sicilian Basin." *Hydrological Processes* 12: 701–711.

Ferro, V., and M. Minacapilli. 1995. "Sediment Delivery Processes at Basin Scale." *Hydrological Sciences Journal* 40, no. 6: 703–717.

Ferro, V., and P. Porto. 2000. "A Sediment Delivery Distributed (SEDD) Model." *Journal of Hydrologic Engineering, ASCE* 5, no. 4: 411–422.

Ferro, V., P. Porto, and G. Tusa. 1998b. "Testing a Distributed Approach for Modelling Sediment Delivery." *Hydrological Sciences Journal* 43, no. 3: 425–442.

Fu, G., S. Chen, and D. K. McCool. 2006. "Modeling the Impacts of No-Till Practice on Soil Erosion and Sediment Yield With RUSLE, SEDD and ArcView GIS." *Soil & Tillage Research* 85: 38–49.

Gessesse, B., W. Bewket, and A. Bräuning. 2015. "Model-Based Characterization and Monitoring of Runoff and Soil Erosion in Response to Land Use/Land Cover Changes in the Modjo Watershed, Ethiopia." *Land Degradation & Development* 26: 711–724.

Jain, M. K., and U. C. Kothyari. 2000. "Estimation of Soil Erosion and Sediment Yield Using GIS." *Hydrological Sciences Journal* 45, no. 5: 771–786.

Kothyari, U. C. 2008. "Soil Erosion and Sediment Yield Modelling." *ISH Journal of Hydraulic Engineering* 14, no. 1: 84–103.

Lal, R. 2014. "Soil Conservation and Ecosystem Services." *International Soil and Water Conservation Research* 2, no. 3: 36–47.

Lane, L. J., M. R. Kidwell, and M. A. Weltz. 2000. "Watershed Sediment Yield and Rangeland Health." *International Journal of Sediment Research* 15, no. 1: 51–59.

Lee, S. E., and S. H. Kang. 2014. "Geographic Information System Coupling Sediment Delivery Distributed Modeling Based on Observed Data." *Water Science & Tecnology* 70: 495–501.

López-Vicente, M., N. Lana-Renault, J. M. García-Ruiz, and A. Navas. 2011. "Assessing the Potential Effect of Different Land Cover Management Practices on Sediment Yield From an Abandoned Farmland Catchment in the Spanish Pyrenees." *Journal of Soils and Sediments* 11: 1440–1455.

Mekonnen, M., S. D. Keesstra, L. Stroosnijder, J. E. M. Baartman, and J. Maroulis. 2015. "Soil Conservation Through Sediment Trapping: A Review." *Land Degradation & Development* 26, no. 6: 544–556.

Moore, I. D., and F. J. Burch. 1986. "Physical Basis of the Length-Slope Factor in the Universal Soil Loss Equation." *Soil Science Society of America Journal* 50: 1294–1298.

Moore, I. D., and J. P. Wilson. 1992. "Length-Slope Factors for the Revised Universal Soil Loss Equation: Simplified Method of Estimation." *Journal of Soil and Water Conservation* 47: 423–428.

Morgan, R. P. C. 2005. *Soil Erosion and Conservation*. 3rd ed, 304. Blackwell.

Morgan, R. P. C., and M. A. Nearing. 2000. "Soil Erosion Models: Present and Future." In *Proceedings of Third International Congress of the European Society for Soil Conservation*, edited by J. L. Rubio, S. Asins, V. Andreu, J. M. de Paz, and E. Gimeno, 145–164. Key Notes Volume (28 March–1 April).

Najafi, S., D. Dragovich, T. Heckmann, and S. H. Sadeghi. 2021. "Sediment Connectivity Concepts and Approaches." *Catena* 196: 104880.

Nearing, M. A. 1997. "A Single Continuous Function for Slope Steepness Influence on Soil Loss." *Soil Science Society of America Journal* 61: 917–919.

Nearing, M. A. 2013. "22—Soil Erosion and Conservation." In *Environmental Modelling: Finding Simplicity in Complexity*, edited by J. Wainwright and M. Mulligan, 2nd ed., 365–378. John Wiley & Sons, Ltd.

Nearing, M. A., G. R. Foster, L. J. Lane, and S. C. Finkner. 1989. "A Process-Based Soil Erosion Model for USDA-Water Erosion Prediction Project Technology." *Transactions of ASAE* 32, no. 5: 1587–1593.

Netti, A. M., F. G. Ricci, O. M. M. Abdelwahab, et al. 2024. "Setting Up the Sediment Delivery Distributed (SEDD) Model: The Carapelle Watershed Case Study." In *Proceedings of 2024 IEEE International Workshop on Metrology for Agriculture and Forestry (MetroAgriFor)*, 387–391. IEEE.

Novotny, V., and G. Chesters. 1989. "Delivery of Sediment and Pollutants From Nonpoint Sources: A Water Quality Perspective." *Journal of Soil and Water Conservation* 44, no. 6: 568–576.

Pampalone, V., A. Nicosia, V. Palmeri, M. A. Serio, and V. Ferro. 2023. "Rill and Interrill Soil Loss Estimations Using the USLE-MB Equation at the Sparacia Experimental Site (South Italy)." *Water* 15: 2396.

Porto, P., and G. Callegari. 2021. "Using ^{7}Be Measurements to Explore the Performance of the SEDD Model to Predict Sediment Yield at Event Scale." *Catena* 196: 104904.

Porto, P., and D. Walling. 2015. "Use of Caesium-137 Measurements and Long-Term Records of Sediment Load to Calibrate the Sediment Delivery Component of the SEDD Model and Explore Scale Effect: Examples From Southern Italy." *Journal of Hydrologic Engineering, ASCE* 20: 1–12.

Raclot, D., Y. Le Bissonnais, M. Annabi, M. Sabir, and A. Smetanova. 2018. "Main Issues for Preserving Mediterranean Soil Resources From Water Erosion Under Global Change." *Land Degradation & Development* 29: 789–799.

Renard, K. G., G. R. Foster, G. A. Weesies, D. K. McCool, and D. C. Yoder. 1997. "Predicting Soil Erosion by Water: A Guide to Conservation Planning With the Revised Universal Soil Loss Equation (RUSLE)." In *USDA Agriculture Handbook*, vol. 703. DC.

Renard, K. G., G. R. Foster, D. C. Yoder, and D. K. McCool. 1994. "RUSLE Revisited: Status, Questions, Answers and the Future." *Journal of Soil and Water Conservation* 49: 213–220.

Richards, K. 1993. "Sediment Delivery and Drainage Network." In *Channel Network Hydrology*, edited by K. Beven and M. J. Kirkby, 221–254. Wiley.

Risse, L. M., M. A. Nearing, A. D. Nicks, and J. M. Laflen. 1993. "Error Assessment in the Universal Soil Loss Equation." *Soil Science Society of America Journal* 57, no. 3: 825–833.

Sadeghi, S. H. R., L. Gholami, M. Homaee, and A. Khaledi Darvishan. 2015. "Reducing Sediment Concentration and Soil Loss Using Organic and Inorganic Amendments at Plot Scale." *Solid Earth* 6: 445–455.

Shi, C., Y. Liang, W. Qin, et al. 2025. "Review of Sediment Connectivity: Conceptual Connotations, Characterization Indicators, and Their Relationships With Soil Erosion and Sediment Yield." *Earth-Science Reviews* 264: 105091.

Taguas, E. V., C. Moral, J. L. Ayuso, R. Pérez, and J. A. Gómez. 2011. "Modeling the Spatial Distribution of Water Erosion Within a Spanish Olive Orchard Microcatchment Using the SEDD Model." *Geomorphology* 133, no. 1–2: 47–56.

Tarquini, S., I. Isola, M. Favalli, A. Battistini, and G. Dotta. 2023. *TINITALY, A Digital Elevation Model of Italy With a 10 Meters Cell Size (Version 1.1)*. Istituto Nazionale di Geofisica e Vulcanologia (INGV). https://doi.org/10.13127/tinitaly/1.1.

Tiwari, A. K., L. M. Risse, and M. A. Nearing. 2000. "Evaluation of WEPP and Its Comparison With USLE and RUSLE." *Transactions of ASAE* 43: 1129–1135.

Todisco, F., L. Brocca, L. F. Termite, and W. Wagner. 2015. "Use of Satellite and Modeled Soil Moisture Data for Predicting Event Soil Loss at Plot Scale." *Hydrology and Earth System Sciences* 19, no. 9: 3845–3856.

Todisco, F., L. Vergni, F. Mannocchi, and C. Bomba. 2012. "Calibration of the Soil Loss Measurement Method at the Masse Experimental Station." *Catena* 91: 4–9.

Todisco, F., L. Vergni, S. Ortenzi, and L. Di Matteo. 2022. "Soil Loss Estimation Coupling a Modified USLE Model With a Runoff Correction Factor Based on Rainfall and Satellite Soil Moisture Data." *Water* 14: 2081.

Walling, D. E. 1983. "The Sediment Delivery Problem." *Journal of Hydrology* 65: 209–237.

Walling, D. E. 1988. "Erosion and Sediment Yield Research-Some Recent Perspectives." *Journal of Hydrology* 100: 113–141.

Walling, D. E., S. B. Bradley, and C. P. Lambert. 1986. "Conveyance Losses of Suspended Sediment Within a Floodplain System." In *Drainage Basin Sediment Delivery*, edited by R. F. Hadley. IAHS Publication (No. 159).

Wischmeier, W. H., C. Johnson, and B. Cross. 1971. "A Soil Erodibility Nomograph for Farmland and Construction Sites." *Journal of Soil and Water Conservation* 26, no. 3: 189–193.

Wischmeier, W. H., and D. D. Smith. 1978. *Predicting Rainfall-Erosion Losses—A Guide to Conservation Farming*. U.S. Department of Agriculture, Agriculture (Handbook No. 537).